Poster 21: LiSyM Midterm Evaluation 2018 Glanemann/Lammert Group (Homburg)

Facts & Figures:

Area of Expertise:	Gastroenterology, hepatology, molecular genetics, randomised controlled clinical trials
Laboratory methods:	Genetic mouse models, histopathology, expression profiling by RT-PCR and ELISA, determination of hepatic collagen content by hydroxyproline assay and collagen area calculation, genotyping, sequencing, isolation of primary murine hepatic cells, cell culture
Scientific involvement:	Pillar III
LiSyM resources:	297.000 €
LiSyM scientists:	[0] PhD Student, [1] PostDoc (Ersin Karatayli), [1] Technical Assistant/StudyNurse (Irina Nowak)
Collaborations:	Steven Dooley from Pillars II&III, Ursula Klingmüller from Pillars II&III, Jan Hengstler from Pillar III, Matthias König from Pillar IV

Setting up clinical cohort patients with ACLF

To set up a clinical cohort of patients with ACLF for LiSyM (Figure 1), we recruited patients with end-stage liver disease (liver cirrhosis) within the framework and screening efforts for two randomized controlled trials, INCA (Figure 2) and GRAFT (Figure 3), which are also supported by BMBF and DFG, respectively. In the INCA screening cohort (N = 750 patients with ACLF; mean age 65 years, 55% alcoholic cirrhosis, 73% decompensated liver cirrhosis) (Table 1), a significant association of bacterial infections as triggers of ACLF was found to be markedly stronger in patients with ACLF as compared to patients with compensated cirrhosis with no ACLF. Together with our LiSyM partners, we modelled the independent predictors for ACLF (type 3) in decompensated cirrhosis; the current model includes clinical, chemical and genetic markers (*NOD2*) as well as liver stiffness (LS) determined by elastography (LS to spleen ratio as indicator of portal pressure) (Table 2). Of note, the presence of *NOD2* risk variants increased the risk of infection five-fold in compensated patients, whereas in ACLF the increase in the risk of infection conferred was two-fold lower, indicating adaptation of the immune system.
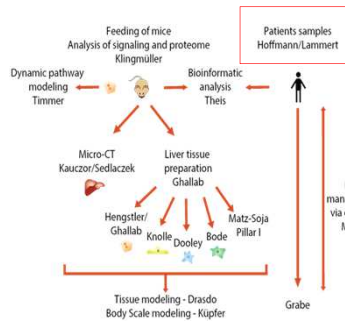

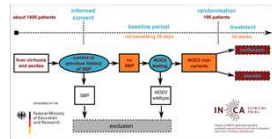
Figure 1. LiSyM pilot experiment scheme

Figure 2. INCA study design (Impact of NOD2 genotype-guided antibiotic prevention on survival in patients with liver Cirrhosis and Ascites)

Table 1. INCA Screening Cohort (N = 2.250)

Parameter	Total (N=750)
Age (years)	61.00 (53.00-68.00)
Gender (male)	487 (64.9%)
NOD2 risk allele (pos)	164 (21.9%)
MELD (points)	10.8 (8.28-14.89)
CPS (points)	6.0 (5-17)
HCC (yes)	92 (12.3%)
Varices (yes)	381 (50.8%)
Etiology of cirrhosis	
Alcoholic	415 (55.3%)
NASH	53 (7.1%)
Hepatitis C	109 (14.5%)
Hepatitis B	22 (2.9%)
Others	76 (10.1%)
Cryptogenic	75 (10.0%)
Decompensation	544 (72.5%)
Ascites (yes)	403 (53.7%)
HE (yes)	144 (19.2%)
VB (yes)	107 (14.3%)
Jaundice (yes)	230 (30.7%)
Bacterial infections	
compensated	35 (17.0%)
decompensated	243 (44.7%)

Values are given as median and interquartile range (IQR) or frequencies and percentages.

Table 2. Models identifying independent predictors for ACLF type 3/ infections in decompensated cirrhosis

Variables introduced	N=	Final model	OR	95% CI	P-Value	AIC
Alb, Ascites, Bilirubin, Creatinin, Hb, HE, INR, Jaundice, LSPS, MELD, NOD2, PTT, Spleen size	240	Alb	0.87	0.76-0.99	0.03	310.7
		HE	2.04	1.06-3.92	0.03	
		Creatinin	1.48	0.87-2.52	0.15	
		Jaundice	2.20	1.24-3.88	0.01	
		NOD2	2.52	1.27-5.02	0.01	
		Spleen size	1.22	1.20-1.37	0.001	
Alb, Ascites, Hb, HE, Jaundice, LSPS, MELD, NOD2, Spleen size, Jaundice	258	Hb	0.83	0.74-0.94	0.004	325.7
		HE	1.90	1.00-3.61	0.05	
		Jaundice	2.34	1.35-4.04	0.002	
		NOD2	2.80	1.44-5.45	0.002	
		Spleen size	1.23	1.10-1.37	0.001	
Alb, Ascites, Bilirubin, Creatinin, Hb, HE, INR, Jaundice, LSPS, NOD2, Spleen size	258	Hb	0.83	0.74-0.94	0.004	327.1
		HE	1.90	1.00-3.61	0.05	
		Jaundice	2.34	1.35-4.04	0.002	
		NOD2	2.80	1.44-5.45	0.002	
		Spleen size	1.23	1.10-1.37	0.001	
Alb, Ascites, Bilirubin, Creatinin, Hb, HE, INR, Jaundice, MELD, NOD2, PTT, Spleen size	410	Alb	0.97	0.94-1.00	0.09	518.0
		Creatinin	1.60	1.09-2.37	0.02	
		Hb	0.85	0.77-0.96	0.001	
		HE	1.53	0.94-2.49	0.09	
		Jaundice	2.16	1.40-3.34	0.001	
		NOD2	1.85	1.11-3.08	0.02	
		Spleen size	1.12	1.04-1.21	0.004	

Abbreviations: AIC, Akaike information criterion; Alb, Albumin; BI, bacterial infection; CPS, Child-Pugh-Score; CSPH, clinically significant portal hypertension variable; Hb, hemoglobin; HE, hepatic encephalopathy; LSPS, liver stiffness to spleen/platelet score; MELD-Score, Model of end stage liver disease; NASH, non-alcoholic steatohepatitis; NOD2, carrier of NOD2 risk allele; OR, Odds ratio; PTT partial thromboplastin time; VB, variceal bleeding; 95% CI: 95% confidence interval.

In a subgroup of ACLF patients (N = 86 until 01/2018), the impact of granulocyte-colony stimulating factor (G-CSF), 30 - 48 Mio. IU OD for one week and then every 3 days until d26) (Figure 3) is being assessed, together with systematic sampling of liver tissue and serum biomarkers. G-CSF mobilised stem as well as immune cells and improved liver function in preclinical trials, hence it represents a yardstick for future treatment design for patients with ACLF within the LiSyM network.
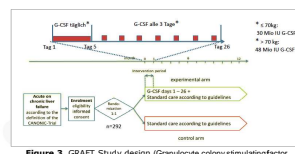

Figure 3. GRAFT Study design (Granulocyte colony stimulating factor (G-SCF) to treat acute on chronic liver failure: A multicenter randomized trial)

To assess future implications of our results in computational models, we summarized the current large-scale computational models of liver metabolism in a review in Hepatology, supported by LiSyM (Cvitanovic et al. 2017). Additionally, current evidence on predictive genomic markers in cholestatic liver diseases including our own prior data was summarized in another LiSyM-funded review (Reichert et al. 2017).

Translational studies and identification of prognostic markers

To identify prognostic markers, the diagnostic performance of three serum markers identified in the preclinical and *in vitro* models (cooperation with P4 U. Klingmüller) was evaluated in terms of liver histology and stiffness in a total of N = 834 patients with chronic liver disease. A significant correlation was found between concentrations of three markers (HGF, GDF-15 and PLGF) and histopathology and liver stiffness (LS), suggesting this panel for non-invasive prediction of disease progression. Cut-offs for advanced liver fibrosis (≥F2) were found to be 2,598 pg/ml, 1,584 pg/ml and 20.2 pg/ml for HGF, GDF-15 and PLGF, respectively (Table 3). An increase of odds ratios from 3.6 over 33.0 to 108.4 with incremental markers positive for LS ≥ 12.8 kPa (all P<0.05) was confirmed by logistic regression analysis (Krawczyk et al. 2017).

Table 3. Determination of AUCs and cut-offs of serum markers according to histological fibrosis stages in the test cohort.

Histological fibrosis stages	Marker	AUC	CI	Cut-off
<F1 vs ≥F1	PLGF*	0.748	0.636-0.861	18.1
	GDF15*	0.839	0.767-0.911	902.5
	HGF*	0.862	0.802-0.922	1821.3
<F2 vs ≥F2	PLGF*	0.758	0.692-0.823	20.2
	GDF15*	0.854	0.808-0.900	1582.8
	HGF*	0.849	0.802-0.898	2598.0
< F3 vs. ≥F3	PLGF*	0.771	0.710-0.832	21.9
	GDF15*	0.901	0.865-0.938	1563.7
	HGF*	0.888	0.848-0.928	2085.7
<F4 vs F4	PLGF*	0.751	0.690-0.813	23.6
	GDF15*	0.898	0.860-0.935	1822.1
	HGF*	0.899	0.861-0.938	2724.9

AUC: Area under the curve, CI: confidence interval;
*P< 0.05

In a subgroup of patients (N=15), we compared LS to ^{13}C-methacetin-based breath tests (LiMAx) in patients undergoing portosystemic shunt intervention to reduce portal pressure (cooperation with pillar IV). LiMAx (which represents CYP1A2 activity) decreased significantly from 301±180 at baseline and 263±127 at intervention to 151±99 μg/kg/h at d14, pointing to a potential prognostic relevance of dynamic liver function tests to guide individualized treatment in decompensated liver cirrhosis (Malinowski et al. 2017).

Animal model of alcohol-induced ACLF

Since in INCA & GRAFT cohorts, alcoholic liver disease is the predominant aetiology of ACLF, we opted to extend the preclinical model with pre-existing liver injury due to deficiency of the hepatobiliary phosphatidylcholine transporter (*Abcb4*-/- mice), which shows spontaneous liver fibrosis, with ethanol challenge as standardized in the NIAAA protocol (Nat Protoc 2013). In the experimental set-up, ten (n=64) and 15 (n=64) week-old wild-type C57BL/6J and *Abcb4* knock-out mice were either fed control or liquid ethanol diet (5% v/v), followed by an acute ethanol binge (5 mg/kg). Phenotypic characterization included hepatic expression profiling by qRT-PCR, ELISA, hepatic collagen contents and histopathology.

In this model, we found that an acute inflammatory IL6-driven response promotes the transition from the stable chronic disease state to progressive injury in *Abcb4*-/- mice (Figure 4A, lower panel).
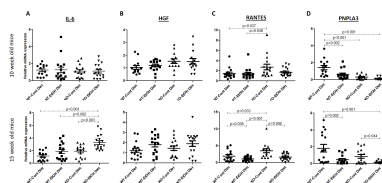

Moreover, metabolic dysregulation and inflammation was also evident by altered RANTES (CCL5) and PNPLA3 (adiponutrin) expression (Figure 4C and 4D, respectively).
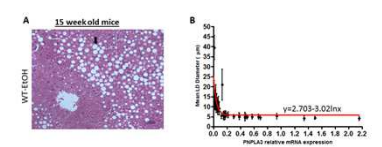
Figure 4. Relative quantification of mRNA levels in liver. Hepatic transcriptional levels of *Il-6* (A), *Hgf* (B), *Rantes* (C) and *Pnpla3* (D) were determined by qPCR in 10 (upper panel) and 15 weeks old mice (lower panel). p<0.05 was considered significant. IL-6; interleukin 6, HGF; hepatocyte growth factor, RANTES; regulated on activation, normal T cell expressed and secreted, PNPLA3; patatin-like phospholipase domain-containing 3, WT; C57BL/6J wild type mice, KO; Abcb4 knock-out mice, EtOH; Ethanol diet, CONT; Control diet.

Of note, non-linear regression analysis demonstrated that the hepatic repression of PNPLA3 resulted in a notable expansion of lipid droplet size after ethanol challenge, suggesting a key role for lipid remodelling in this setting (Figure 5).

Figure 5. Formation of lipid droplets. Hepatic steatosis was observed in ethanol challenged mice regardless of the genotype as shown by accumulation of lipid droplets observed in representative H&E stained histological slices (A). Repression of *pnpla3* expression resulted in a notable expansion of lipid droplet size as demonstrated by a non-linear regression analysis estimating a correlation formula of "*mean LD size(μm) = 2.703 − 3.02 ln[relative PNPLA3 mRNA level]*" (r2= 0.46 and p<0.01). LD; lipid droplet, PNPLA3; patatin-like phospholipase domain-containing 3, WT; C57BL/6J wild type mice, KO; Abcb4 knock-out mice, EtOH; Ethanol diet, CONT; Control diet. Scale bar is 100 μm. Magnification 20X.

Publications:

1. Cvitanovic et al. Large-scale computational models of liver metabolism: How far from the clinics? *Hepatology* 2017;66:1323-1334.
2. Krawczyk et al. Panel of three novel serum markers predicts liver stiffness and fibrosis stages in patients with chronic liver disease. *PLoS One* 2017;16;12(3).
3. Reichert et al. Genetic determinants of cholangiopathies: molecular and systems. *Biochim Biophys Acta* 2018;1864:1484-1490.
4. Jamka et al. Effects of gene variants controlling vitamin D metabolism and serum levels on hepatic steatosis. *Digestion* 2018;97:298-308.
5. Krawczyk et al. Could inherited predisposition drive non-obese fatty liver disease? Results from German tertiary referral centers. *J Hum Genet* 2018 (epub ahead of print)
6. Reichert et al. Common NOD2 risk variants have differential effects on bacterial infections in compensated and decompensated stage of cirrhosis (submitted to *Hepatology* 2018)
7. Karatayli et al. Effect of alcohol on the IL-6 mediated inflammatory response in a new mouse model of acute-on-chronic liver injury (submitted to *Biochim Biophys Acta* 2018)